JOURNAL OF SOLID STATE CHEMISTRY 66, 144–153 (1987)

Structural and Electronic Properties of γ-$Tl_2Cu(SO_4)_2$

R. DURNÝ,* D. BARANČOK, AND J. WEIS

Department of Physics, Slovak Technical University, Mlynská dolina, 812 19 Bratislava, Czechoslovakia

AND H. LANGFELDEROVÁ AND M. SERÁTOR

Department of Inorganic Chemistry, Slovak Technical University, Jánska ul. 1, 811 07 Bratislava, Czechoslovakia

Received December 16, 1985; in revised form April 10, 1986

The compound $Tl_2Cu(SO_4)_2$, belonging to the dehydrated copper Tutton salts [$Cat_2Cu(SO_4)_2$, where Cat stands for cation], and especially its glassy γ-modification was investigated. The results of X-ray diffraction analysis, electron paramagnetic resonance, differential thermal analysis, electrical conductivity, and thermostimulated depolarization measurements are presented and discussed. An evident correlation among the results of various experimental techniques was found.

1. Introduction

Since the discovery of switching phenomena (*1*), amorphous semiconductors have received much attention due to their great potential in xerography, solar cells, memory and switching devices, amorphous/crystalline heterojunctions, etc. (*2*).

It also seems reasonable to study some coordination compounds from the point of view of their utilization in materials science. Depending on the conditions of preparation, coordination compounds can be prepared in single crystal, polycrystalline, or amorphous form. From the dehydrated copper Tutton salts (general formula $Cat_2Cu(SO_4)_2$, where Cat stands for cation) the compound $Tl_2Cu(SO_4)_2$ and especially its amorphous γ-modification was investigated. Since the above-mentioned compound exhibits semiconductor properties we have in fact dealt with an amorphous semiconductor.

Here, we present the results of X-ray diffraction analysis, electron paramagnetic resonance (EPR), differential thermal analysis (DTA), preliminary both electrical conductivity, and thermostimulated depolarization (TSD) measurements performed on amorphous γ-$Tl_2Cu(SO_4)_2$.

2. Experimental

The α-, β-, and γ-$Tl_2Cu(SO_4)_2$ were prepared under controlled conditions from the dehydrated melt of $Tl_2Cu(SO_4)_2$. Slow cooling ($\sim$10°C min^{-1}) led to a blue–green flaky crystalline modification (α-), rapid cooling of the melt to $\sim$100°C and slow gradual cooling to room temperature led to the β-

* To whom correspondence should be sent.

0022-4596/87 $3.00

form and the product of a rapid cooling to room temperature was the glassy[1] γ-modification. The structural differences among the α-, β-, and γ-$Tl_2Cu(SO_4)_2$ have already been investigated using spectral methods and powder diffraction (*3*).

The structure of glassy γ-$Tl_2Cu(SO_4)_2$ sample was tested by both X-ray diffraction analysis and DTA. All the samples under investigation were glassy, no crystalline regions occurred except at the surface regions of samples contaminated by atmospheric humidity.

DTA of the powdered samples was carried out on a Dupont Thermal Analyzer 900, provided with a high temperature cell, up to 400°C. A small amount (30 mg) of glass was placed in a corundum pan, using recrystallized α-Al_2O_3 powder as a reference material, and the measurements performed at a heating rate of 10°C min^{-1} under low argon overpressure.

X-Ray analysis was performed using TUR-M-62 apparatus. The X-ray intensities were collected in the transmission geometry by a flat graphite monochromator in the diffracted beam. All experimental data were obtained by Mo*K* radiation within a scattering angle range of $5° < \theta < 70°$, i.e., for $15.4 \leq K \leq 166$ nm^{-1} ($K = (4\pi/\lambda) \sin\theta$, where λ is the X-ray wavelength). The range of scattering angles was covered using a step length of 0.1° for $\theta \leq 20°$, 0.2° for $20° \leq \theta \leq 40°$, and 0.4° for $40° < \theta \leq 70°$. The intensities were subsequently corrected for background, polarization, absorption, and Compton scattering. The residual fluorescent radiation of the samples could be eliminated from the measured intensity by an appropriate choice of lower treshold voltage for the measuring channel. The intensities were normalized to electron units using an analytical radial distribution function (RDF) method (*4*). The total interference functions were calculated using the relation

$$I(K) = \frac{I_a(K) - \langle f^2\rangle + \langle f\rangle^2}{\langle f^2\rangle} \qquad (1)$$

where $I_a(K)$ is the scattering intensity per atom, $\langle f^2\rangle = \Sigma_i\, c_i f_i(K) f_i^*(K)$, $\langle f\rangle^2 = \Sigma_i \Sigma_j\, c_i c_j f_i(K) f_j^*(K)$, and c_i, $f_i(K)$ are, respectively, the concentration and scattering factor of element i. Radial distribution functions RDF(r) were calculated using

$$\mathrm{RDF}(r) = 4\pi r^2\rho_0 + \frac{2r}{\pi}\int_0^{K_{max}} K[I(K) - 1]\exp(-BK^2)\cdot\sin(Kr)dK \qquad (2)$$

where ρ_0 is the mean atomic number density, B is a damping factor which reduces ghost ripples due to the termination of $I(K)$ and is usually chosen so that $\exp(-BK_{max}^2) = 0.1$. We used the value $B = 9 \times 10^{-5}$ nm^2. The intensity data observed at K values smaller than K_{min} were smoothly extrapolated to the value $K = 0$ nm^{-1}.

The EPR spectra were recorded using a Varian E-4 spectrometer operating in the X-band at 100 kHz field modulation. The glassy samples were either crushed or powdered and several chunks (or powder) put into an EPR sample tube. The EPR spectra of copper(II) complexes may be measured in two ways: as polycrystalline powders or as single crystals (*5*). The former technique is the most rapid experimentally but only yields approximate g-values (*6*), and the results may be subject to misinterpretation. The factors which determine the type of EPR spectrum observed are:

(a) the nature of the electronic ground state;

(b) the symmetry of the effective ligand-field about the copper(II) ion;

(c) the mutual orientations of the local molecular axes of the separate copper(II) chromophores in the unit cell.

The measurement of EPR spectra gives the most precise information on the electronic

[1] Glassy material means an amorphous one which exhibits glass transition.

ground state—a distinction between a $d_{x^2-y^2}$ and a d_{z^2} ground state. The latter is indicated by a low g-value ($g < 2.04$), the former by an axial (or approximately axial, $g_1 \approx g_2 = g_\perp$) spectrum with $G = (g_\parallel - 2/g_\perp - 2)$ (*8*) approximately equal to 4.0. If $G > 4.0$, then local tetragonal axes are aligned parallel or only slightly misaligned, if $G < 4.0$ significant exchange coupling is present (*7*). Consequently the value of G is a useful indication of the extent of exchange coupling in tetragonal systems. If all tetragonal axes are aligned parallel then the crystal g-values accurately reflect the local copper (II) ion environment g-values, and these may be measured using either single crystal techniques or (slightly less accurately) by measurements upon polycrystalline samples. If the tetragonal axes in the unit cell are not aligned parallel, then the observed crystal g-values are not simply related to g-values of the local copper(II) ion environment (*8*). If the complexes are of known crystal structure then the observed g-values may be related to the local g-values (*9*). It is not possible to specify precisely the local g-values if the crystal structure is unknown.

The electrical conductivity measurements were made using evaporated Au contacts. Prior to the evaporation of metal contacts surfaces of samples were mechanically treated with caution to avoid local heating. We assume the validity of the conduction expression (*10*)

$$\sigma = C \exp\left(-\frac{\Delta E}{kT}\right)$$

where $C = \sigma_0 \exp(\gamma/k)$. Hence, γ stands for the temperature coefficient of the band gap. If the electrical conduction is due to the electrons excited beyond the mobility shoulder E_c into the extended states, ΔE is equal to half band gap extrapolated to zero temperatures $\Delta E = E_c - E_{F_0}$ (E_F—Fermi level). ΔE can be determined from the plot of ln σ versus $1/T$ which should be a straight line.

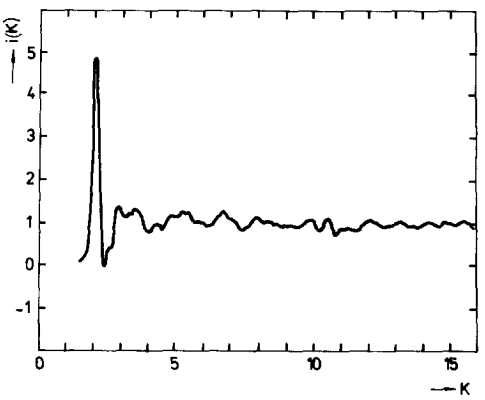

FIG. 1. The interference function of γ-$Tl_2Cu(SO_4)_2$.

In 1970 Kolomiets *et al.* (*11, 12*) proposed to investigate the localized states in the mobility gap of amorphous semiconductors by means of the so-called thermally stimulated depolarization. Two experimental arrangements were used—contacts fitted without metal evaporation, i.e., samples placed between carefully polished metal electrodes (Pt) in order to avoid injection and space-charge effects which would be responsible for enormous high-temperature TSD peaks, and for comparison, a set of experiments were performed with evaporated Au contacts.

3. Results

3.1. X-Ray Diffraction Analysis

The interference function of glassy γ-$Tl_2Cu(SO_4)_2$ is shown in Fig. 1. Contrary to the interference functions of metallic glasses this function exhibits a pronounced structure at high values of K and the position of the first maximum is at a relatively low value of $K \sim 20$ nm^{-1}. Radial distribution functions of γ-$Tl_2Cu(SO_4)_2$ are shown in Fig. 2: the reduced function $G(r) = 4\pi r[\rho(r) - \rho_0(r)]$ and the atomic function $\mathrm{RDF}(r) = 4\pi r^2\rho_0 - rG(r)$, where $\rho(r)$ is the

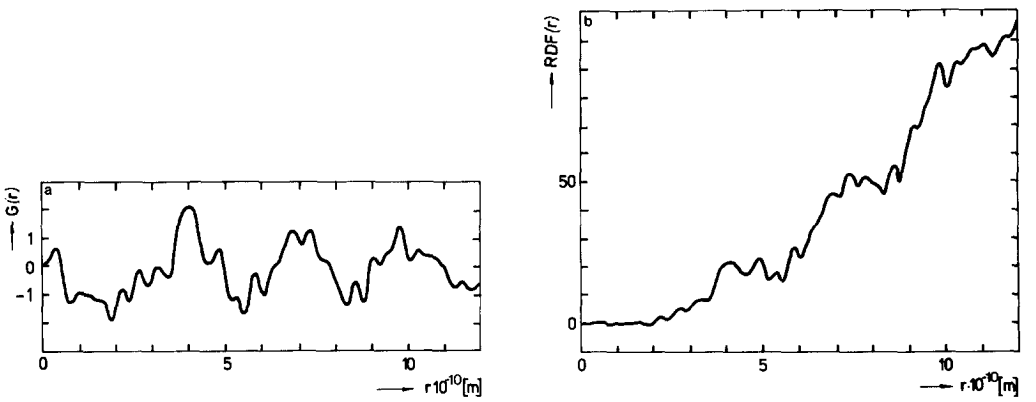

FIG. 2. Radial distribution functions of γ-$Tl_2Cu(SO_4)_2$.

so-called overall radial distribution function. These functions, in comparison with the radial distribution functions of metallic glasses, are more pronouncedly modulated: this is the demonstration of the high degree of short range order. The main maximum of the first coordination sphere is located at a relatively large distance of $r = 0.4$ nm. The sphere-to-sphere distances are surprisingly large. Due to the expected complicated structure of the short range order we shall confine our discussion to the main maximum of both RDF(r) and $G(r)$. Table I shows both the submaximum positions in the first coordination sphere and the coordination numbers calculated according to

$$Z = \int_{r_1}^{r^2} \mathrm{RDF}(r)dr$$

3.2. *EPR and DTA Measurements*

At room temperature, a deformed asymmetric signal was found, centered at $g = 2.172$ with a linewidth ΔH (peak-to-peak of the first derivative of the absorption line) of 520 G. EPR measurements in the temperature range 298 to 77 K (Fig. 3) show no substantial difference between g-values, linewidths, and lineshapes of the signal at room temperature and those at 77 K. However, the increase of temperature changes the shape of the measured spectrum and at $\approx$80°C a deformed axial spectrum was observed, characterized by $g_\perp = 2.08$ and $g_\parallel = 2.41$ (Fig. 3). The axial features of the measured spectrum are preserved for temperatures up to $\approx$140°C. Above this temperature the line gradually becomes isotropic and nearly Gaussian: a further increase in temperature results in its decreasing intensity. At $\approx$175°C a narrowing of the line is observable, and its intensity increases, reaching a maximum at $\approx$200°C. Above this temperature, the EPR line again broadens and decreases in intensity.

In order to compare the EPR signals of various modifications Figs. 4 and 5 show the development, with temperature, of the EPR spectra of α-$Tl_2Cu(SO_4)_2$ (the stablest crystalline modification) and β-Tl_2Cu

TABLE I

SUMMARY OF RESULTS OF THE RDF ANALYSIS

$$\left(Z_i = \int_{i-1}^{i} \mathrm{RDF}(r)dr,\ Z = \sum_{i=1}^{6} Z_i\right)$$

Submaximum (i)	1	2	3	4	5	6
Positions of maxima						
$G(r)$ [nm]	0.21	0.26	0.32	0.40	0.48	0.53
r [nm]	0.2	0.23	0.28	0.34	0.45	0.51
r [nm]	0.23	0.28	0.34	0.45	0.51	0.56
Coordination number Z_i	0.54	1.99	4.27	13.42	11.6	6.56
Total coord. number	$Z = 44.4$					

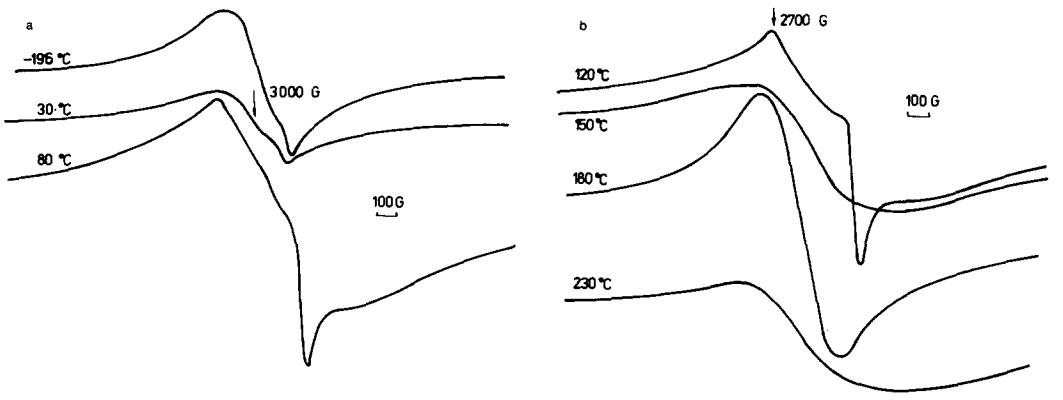

FIG. 3. EPR spectra of γ-$Tl_2Cu(SO_4)_2$ in the temperature range from −196 to 230°C.

$(SO_4)_2$, respectively. At room temperature the α-modification produces an asymmetric line characterized by $g = 2.18$ and linewidth ΔH of 385 G. The decrease of temperature to 77 K does not lead to the qualitative changes in the parameters of the spectra. However, at ≈80°C the asymmetric EPR line changes to an axial spectrum with $g_\parallel = 2.40$ and $g_\perp = 2.08$. The axial character of the spectrum is preserved up to 160°C when an isotropic, nearly Lorentzian line appears. A further increase in temperature results in the broadening and decreasing intensity of the line. Above ≈200°C the line gradually fades out.

With respect to the β-modification, the development with temperature of the EPR spectrum is shown in Fig. 5. At room temperature an isotropic Lorentzian line with $g = 2.18$ and a linewidth ΔH of 345 G is observed. There is no significant difference between the EPR spectrum at room temperature and that at 77 K. With increasing temperature a deformed spectrum, in which axial features can be anticipated, is preserved up to ≈160°C. Further increase of temperature yields an isotropic, again Lorentzian, line that gradually broadens out.

The typical DTA curve of the glassy γ-

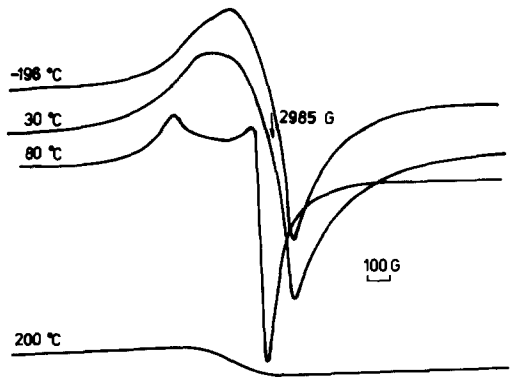

FIG. 4. EPR spectra of α-$Tl_2Cu(SO_4)_2$ in the temperature range from −196 to 200°C.

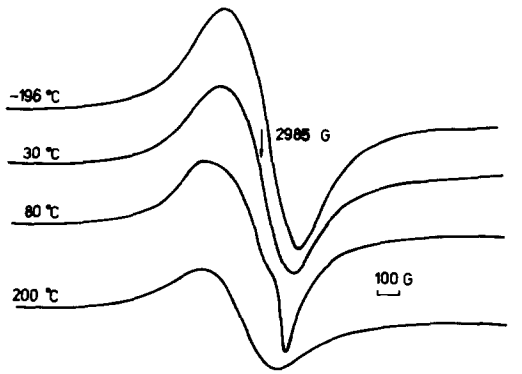

FIG. 5. EPR spectra of β-$Tl_2Cu(SO_4)_2$ in the temperature range from −196 to 200°C.

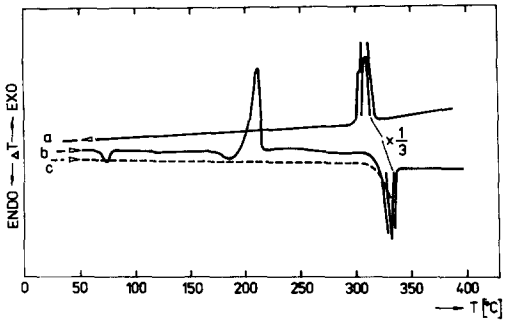

FIG. 6. DTA curve of γ-$Tl_2Cu(SO_4)_2$.

$Tl_2Cu(SO_4)_2$ is shown in Fig. 6. Although the exo-peak at 215°C (T_g) corresponding to the transition from glassy to crystalline state dominates the DTA record there are also two minor endo-peaks at 75 and 185°C. The melting temperature of γ-$Tl_2Cu(SO_4)_2$ is 334°C.

3.3. *Electrical Conductivity Measurements*

The measurements were performed using a relatively simple apparatus. Evaporated gold contacts in a guarded configuration were used because of the high room temperature electrical resistivity of the samples.

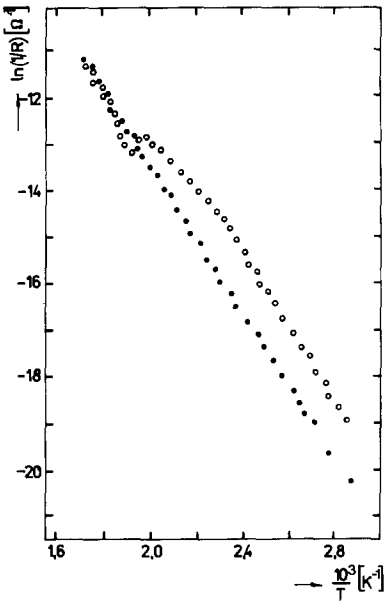

FIG. 7. Electrical conductivity of "virgin" γ-$Tl_2Cu(SO_4)_2$ as a function of temperature.

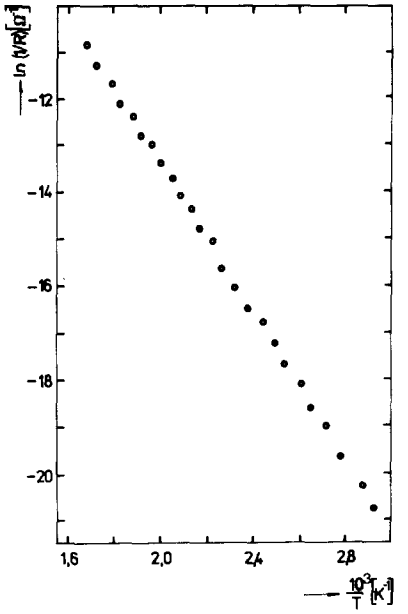

FIG. 8. Electrical conductivity of annealed γ-$Tl_2Cu(SO_4)_2$ as a function of temperature.

The results of conductivity measurements on (a) "virgin" samples of glassy γ-$Tl_2Cu(SO_4)_2$, and (b) a sample of γ-$Tl_2Cu(SO_4)_2$ previously annealed above its T_g in the temperature range from room temperature to 280°C are shown in Figs. 7 and 8 (the plots of $\ln(1/R)$ versus $1/T$), respectively.

The isothermal measurements on γ-$Tl_2Cu(SO_4)_2$ at 50, 110, and 215°C give the results shown in Fig. 9.

3.4. *TSD Measurements*

The TSD currents were measured in a cryostat of our own construction (Fig. 10). The experimental procedure is based on the measurement of the discharging current from an Au–γ-$Tl_2Cu(SO_4)_2$–Au structure, previously polarized for a time interval t_p in darkness at a temperature T_p, with subse-

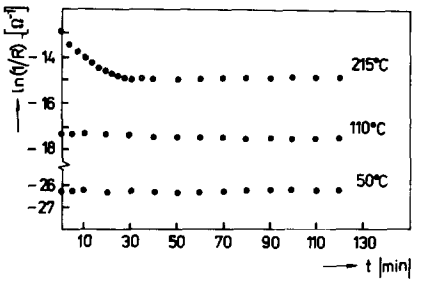

FIG. 9. Isothermal measurements of electrical conductivity of γ-$Tl_2Cu(SO_4)_2$.

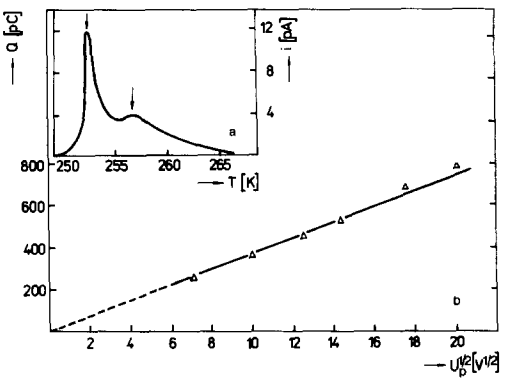

FIG. 11. (a) Typical i–T thermogram for γ-$Tl_2Cu(SO_4)_2$. (b) Total charge released during TSD measurements as a function of the polarizing voltage.

quent cooling of the system with applied voltage U_p to ~80 K. At this temperature the voltage is removed and the system is short-circuited by an electrometer. During heating at a linear rate, β, thermostimulated currents were recorded (i–T thermograms). A typical i–T thermogram is shown in Fig. 11a. It should be noted that no difference was observed between the results of TSD measurements in either experimental arrangement (see Experimental).

The dependence of the total charge released during TSD measurements on polarizing voltage is shown in Fig. 11b.

4. Discussion

The interpretation of the RDF(r) of glassy γ-$Tl_2Cu(SO_4)_2$ is complicated because of the great number of constituent atoms. It is reasonable to expect that in the first coordination sphere not only the interactions of the heavy elements (Tl–Cu, Tl–S, Cu–S), but also the interactions inside the SO_4 group (S–O, O–O) as well as those of oxygen with other elements will manifest themselves. On the other hand, the fact that the SO_4 groups are relatively independent structural units can facilitate the interpretation. It is also clear that the direct Cu^{2+}–Cu^{2+}, Tl^{+}–Tl^{+}, and SO_4^{2-}–SO_4^{2-} interactions should be excluded. On the basis of the above-mentioned facts we propose the structural model shown in Fig. 12 which, to a first approximation, can be derived from an octahedral unit with a central Cu^{2+} ion.

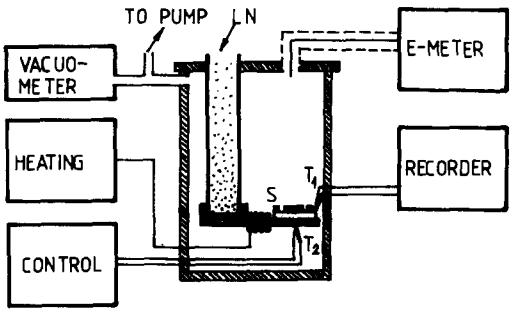

FIG. 10. A schematic picture of the experimental arrangement used.

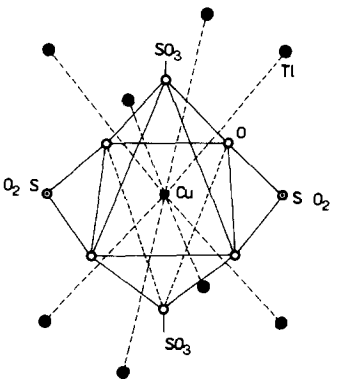

FIG. 12. Structural model of γ-$Tl_2Cu(SO_4)_2$.

The starting point of our model was the structure of the hexaaquacopper(II) in $Tl_2Cu(SO_4)_2 \cdot 6H_2O$ (*13*). It is reasonable to expect that the glassy γ-phase prepared by thermal decomposition of the hexaaquacopper(II) consists of the structural units preserving the basic octahedral stereochemistry, although it is probable that the dehydration has led to a change in the Cu–O distance. This assumption is confirmed by the ligand-field spectrum of this compound (*3*) and by the fact that g-values characterizing the axial spectrum of γ-$Tl_2Cu(SO_4)_2$ ($g_\perp = 2.08$, $g_\parallel = 2.41$) do not differ appreciably from those of the single crystal Tutton salt $Tl_2Cu(SO_4)_2 \cdot 6H_2O$ ($g_x = 2.0704$, $g_y = 2.1161$, $g_z = 2.4180$) (*14*). It means that there is probably a minor change only in the symmetry of the effective ligand field about the copper(II) ions in the above-mentioned compounds.

On the basis of our model (Fig. 12) we interpret the first submaximum (Table I) as Cu–O and O–O interactions and the second submaximum as Cu–S interactions. Elements with a great number of electrons (Tl, Cu, S) have the most pronounced effect on the distribution functions, therefore in the first coordination sphere the Tl–Tl and Tl–Cu interactions probably play the dominant role. It is for this reason that main submaximum of the RDF(r) at $r = 0.4$ nm was ascribed to these interactions. Along the vertical directions the SO_4 groups enter the bond with the central Cu^{2+} ion through an oxygen atom and probably bridge the neighboring arrays of $Tl_2Cu(SO_4)_2$. As the Cu^{2+}–SO_4 distances along the vertical and horizontal directions are different we can also expect a dispersion in the values of the Cu–S distances. Taking into account the deformation of the real structure we interpret the third submaximum as the result of the Tl–S interaction.

It should be noted that the above-mentioned interpretation of the measured submaxima is not the only possible one.

The study of structural changes after annealing at various temperatures from 50 to 210°C reveals that the crystallization of γ-$Tl_2Cu(SO_4)_2$ is a very complicated process and on the basis of our X-ray diffraction measurements it is impossible to unanimously state that the transformation from glassy to crystalline state starts with the precipitation of the α-phase only, and that the product of crystallization is the pure α-$Tl_2Cu(SO_4)_2$.

The reason for observing a deformed isotropic EPR spectrum up to ≈80°C is probably the extensive exchange coupling between the grossly misaligned tetragonal axes of copper(II) ions and the structural disorder in γ-$Tl_2Cu(SO_4)_2$. The misalignment is the result of the freezing of copper (II) coordination polyhedric axes in random but defined positions during the preparation of samples. The increasing temperature intensifies the thermal motion and at ≈80°C tetragonal axes becomes aligned parallel or only slightly misaligned (see also the endo-peak at ≈75°C in the DTA record). The result is an axial spectrum with $G > 4.0$ (the exact value of G for γ-$Tl_2Cu(SO_4)_2$ is $G_\gamma = 5.125$), which indicates the $d_{x^2-y^2}$ electronic ground state of the copper(II) ions. The further development of the line with increasing temperature up to ≈175°C is in accordance to predictions. Due to the increasing intensity of thermal motion tetragonal axes become grossly misaligned and at ≈140°C the spectrum changes its shape from axial to isotropic. The intensity of both the axial and isotropic lines decreases with increasing temperature.

Rather unexpected is the further development of the line. We suppose that both the narrowing of the line and its increasing intensity with increasing temperature is caused by the exchange interaction between similar copper(II) ions which appears at ≈175°C due to a certain structural reorganization in the still glassy γ-

$Tl_2Cu(SO_4)_2$ (see also the endo-peak at ≈185°C in the DTA record).

Our interpretation is based on Van Vleck's theory (*15*). He found that there is no contribution to the second moment from isotropic exchange between similar ions, but that there is a contribution to the fourth moment. This suggests that central part of the line will be narrowed and the excess area distributed in the wings. That is, the line will be peaked and becomes Lorentzian. This phenomenon is known as "exchange narrowing." There are, however, other circumstances under which isotropic exchange does not cause narrowing. Using the more complex theory of Pryce and Stevens (*16*), we can conclude that the exchange does make a contribution to the second moment. It is therefore necessary to decide under what conditions the resonance line will broaden, or narrow.

TSD and dc electrical conductivity measurements were performed in the hope of getting insight into the mechanism of electrical transport in the investigated glassy γ-$Tl_2Cu(SO_4)_2$. The electrical conductivity measurements have shown (Fig. 8) that glassy γ-$Tl_2Cu(SO_4)_2$ up to ≈175°C is a semiconductor with electrical activation energy $\Delta E = 0.76$ eV and room temperature specific resistivity $\rho_{RT} = 4.10\ \Omega$ cm. In the temperature range from 175 to 210°C a change in activation energy is observed, $\Delta E = 0.5$ eV. Around T_g, at 210°C, ΔE again acquires its previous value of 0.76 eV. This means that the resulting polycrystalline samples have the same activation energy as glassy ones have up to ≈175°C. This conclusion also follows from the temperature dependence of electrical conductivity of a previously glassy sample annealed at 210°C (1 h) (Fig. 8) which gives an activation energy of 0.75 eV. This value is, within the experimental error, practically the ΔE for "virgin" glassy γ-$Tl_2Cu(SO_4)_2$. Above 210°C the conductivity decreases and reaches minimum at ≈230°C. Further increase of the temperature yields increasing conductivity and the slope of the $\sigma = \sigma(T)$ dependence, i.e., the activation energy approaches its initial value of 0.76 eV.

Isothermal measurements at 50 and 110°C (Fig. 9) have shown that the electrical conductivity remains unchanged, i.e., the glassy γ-$Tl_2Cu(SO_4)_2$ is an electronically conducting glass without an appreciable contribution of ionic conduction to the transport of charge.

The results of our X-ray analysis, EPR, DTA, as well as electrical resistivity measurements on glassy γ-$Tl_2Cu(SO_4)_2$ can be explained on the basis of the assumption that at about 175 ± 10°C this modification undergoes a structural reorganization which precedes the transition from glassy to polycrystalline state. We ascribe the dispersion in the temperatures at which the reorganization occurs to the different heating rates of samples during the corresponding measurements.

Parameters of deep electron traps in glassy γ-$Tl_2Cu(SO_4)_2$ are completely unavailable. Therefore we assume that the analysis of TSD curves will yield valuable information. Figure 11a shows that the TSD curve is composed of two maxima positioned at $T_{m1} = 252.4$ K and $T_{m2} = 256.3$ K, respectively, where T_m is the temperature at the corresponding maximum of a TSD current.

The analysis will be made assuming both TSD peaks to be fairly discrete and assuming first order kinetics with the possibility of independent analysis. Using the initial rise method (*17*) and the very approximate relation of Schade and Herrick (*18*) the TSD activation energies can be obtained. The above methods give, for the T_{m1} peak, the following activation energies: $\Delta E_{TSD} = 0.518$ eV and $\Delta E_{TSD} = 0.522$ eV, respectively. Because of the uncertainty in the decomposition process the TSD activation energy corresponding to T_{m2} peak can not be determined reliably by the initial rise

method. The relation of Schade and Herrick yields for T_{m2} peak the value of ΔE_{TSD} = 0.530 eV. The interpretation of TSD measurements in terms of localized levels in the gap gives two discrete traps, 0.52 and 0.53 eV, in the forbidden band. It should be noted that instead of two discrete energy levels we have probably a narrow band of energies in the gap.

The area under a TSD peak represents the charge Q which flows in the external circuit. The released charge versus polarizing voltage dependence gives valuable information on the mechanism of electrical conduction in the system under investigation. It can be shown that this dependence is linear if ionic conduction dominates the charge transport and quadratic if the samples under investigation are electronically conducting (*19*). As it is evident from Fig. 11b the best fit of the $Q = Q(U_p)$ dependence can be obtained with $Q \sim U_p^{1/2}$. This means that the electrical transport in glassy γ-$Tl_2Cu(SO_4)_2$ is essentially by means of electrons.

5. Conclusions

The applied methods for studying the compound γ-$Tl_2Cu(SO_4)_2$ have shown:

(i) the presence of the $d_{x^2-y^2}$ electronic ground state of the copper(II) ions;

(ii) the axial symmetry of the effective ligand-field about the copper(II) ions;

(iii) an exchange narrowing of the EPR line and its increasing intensity with increasing temperature;

(iv) that γ-$Tl_2Cu(SO_4)_2$ is essentially an electronically conducting amorphous semiconductor with electrical activation energy ΔE = 0.76 eV and with a narrow band of energies (deep levels) in the gap (0.52–0.53 eV);

(v) that at 175 ± 10°C γ-$Tl_2Cu(SO_4)_2$ undergoes a structural reorganization which precedes the transition from glassy to polycrystalline state.

On the basis of X-ray diffraction analysis a structural model of γ-$Tl_2Cu(SO_4)_2$ has been proposed.

References

1. S. R. Ovshinsky, *Phys. Rev. Lett.* **21,** 1450 (1968).
2. Y. Hamakawa, Ed., "Amorphous Semiconductor Technology and Devices," North-Holland, Amsterdam (1984).
3. F. Foret, H. Langfelderová, and J. Gažo, *J. Therm. Anal.* **25,** 487 (1982).
4. C. N. J. Wagner, *in* "Liquid Metals: Chemistry and Physics" (S. Z. Beer, Ed.), p. 257, Dekker, New York (1972).
5. B. R. McGarvey, *Trans. Met. Chem.* **3,** 89 (1966).
6. T. S. Johnston and H. G. Hecht, *J. Mol. Spectrosc.* **17,** 98 (1965).
7. J. C. Eisentein, *J. Chem. Phys.* **28,** 323 (1958).
8. I. M. Procter, B. J. Hathaway, and P. Nicholls, *J. Chem. Soc. A,* 1678 (1968).
9. D. E. Billing and B. J. Hathaway, *J. Chem. Phys.* **50,** 1476 (1969).
10. N. F. Mott and E. A. Davis, "Electronic Processes in Non-Crystalline Materials," Oxford Univ. Press, London/New York (1971).
11. B. T. Kolomiets and T. F. Mazets, *J. Non-Cryst. Solids* **3,** 46 (1970).
12. B. T. Kolomiets, T. N. Mamontova, and A. A. Babajev, *J. Non-Cryst. Solids* **8–10,** 1004 (1972).
13. K. G. Shields, J. J. Van der Zee, and C. H. L. Kennard, *Cryst. Struct. Commun.* **1,** 371 (1972).
14. T. D. Waite and M. A. Hitchman, *Inorg. Chem.* **15,** 2155 (1976).
15. J. H. Van Vleck, *Phys. Rev.* **74,** 1168 (1948).
16. M. H. L. Pryce and K. W. H. Stevens, *Proc. Phys. Soc. London Sect. A* **63,** 36 (1950).
17. C. Bucci, R. Fieschi, and G. Guidi, *Phys. Rev.* **148,** 816 (1966).
18. H. Schade and D. Herrick, *Solid-State Electron.* **12,** 857 (1969).
19. J. G. Simmons and G. W. Taylor, *Phys. Rev. B: Condens. Matter* **6,** 4793 (1972).